Concerning Carbo Compounds: On the Nature of C_2 Units

Frank R. Wagner, Enkhtsetseg Dashjav, Bambar Davaasuren, Guido Kreiner, Walter Schnelle, and Rüdiger Kniep

Introduction

Initially, our studies on rare earth carbometalates of transition metals, $R_xM_yC_z$, were focused on compounds with monoatomic C units only. In the course of our extended studies of these systems we came across with novel compounds like $La_7Os_4C_9$ containing monoatomic and diatomic C_2 units in their crystal structures [1]. This immediately raises the question about the chemical bonding in these units, and their possible classification in terms of simple model systems, i.e., C_2^{2-}, C_2^{4-}, C_2^{6-}.

For this purpose we have chosen to utilize methods based on complete position space partitioning as the QTAIM (quantum theory of atoms in molecules) method [2] and the ELI-D (electron localizability indicator) partitioning. The underlying scalar fields, the electron density and ELI-D [3-6] are physically meaningful quantities, which describe certain aspects of the electronic behavior in position space. They do no explicitly depend on orbitals and basis sets and can, therefore, be evaluated with any kind of basis set (e.g. Gaussian type of basis sets for molecules, plane wave basis sets for solids) at any reasonable level of theory (uncorrelated or correlated). For the present case, the results have been obtained on the basis of the electronic structure given by the LMTO-ASA method using DFT/LDA.

On the other hand, for the characterization of the diatomic units in terms of a bond order, which is most commonly interpreted in terms of MO theory, a COHP analysis is performed as well.

In position space the situation is the following: A suitable way to define bond orders is to employ the delocalization index between two QTAIM basins. Unfortunately, this quantity which depends on the same-spin pair density is yet too complicated to be calculated for solids. The raw ELI-D bond basin populations are not directly related to the formal bond order derived from the difference between the number of occupied bonding and antibonding MOs. It was shown that usage of a suitable reference system may yield effective bond orders which are consistent with interatomic force constants from lattice dynamical models fitted to experimental vibrational spectra [7]. Here, we first of all focus on CaC_2 (tetragonal modification) as the prototype compound for a C_2^{2-} unit.

C_2 in CaC_2

The crystal structure of CaC_2 in its tetragonal modification is easily described as body centred arrangement of Ca atoms and C_2 units in parallel orientation.

Taking into account the MO diagram of C_2^{2-} with discrete orbitals σs, $\sigma^* s$, σp, πp, with only the latter one being two-fold degenerate, the obtained DOS exhibits a remarkably simple structure (Fig. 1a).

At best three different regions (A, B, C) can be identified with B and C already slightly merged. For these regions the partial electron density and

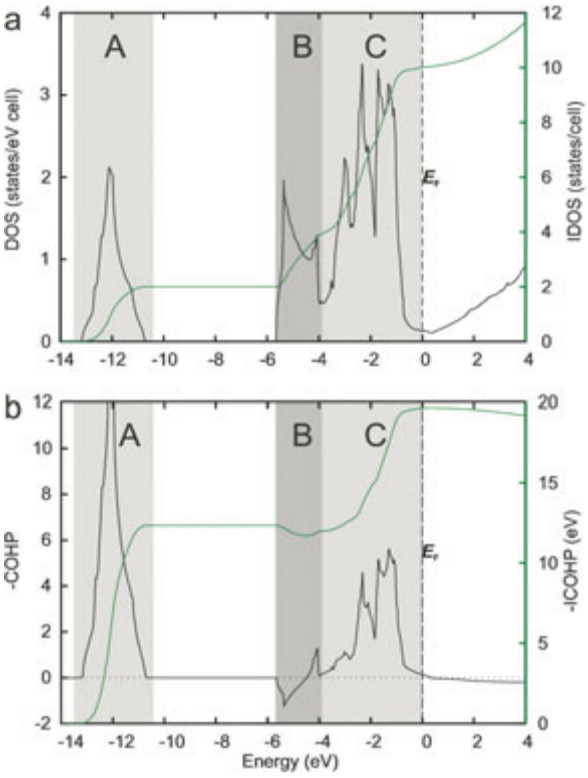

Fig. 1: Tetragonal CaC_2. (a) total DOS and (b) COHP(C–C).

the corresponding pELI-D contributions have been calculated. For comparison the COHP curve for interactions C–C has been calculated as well (Fig. 1b).

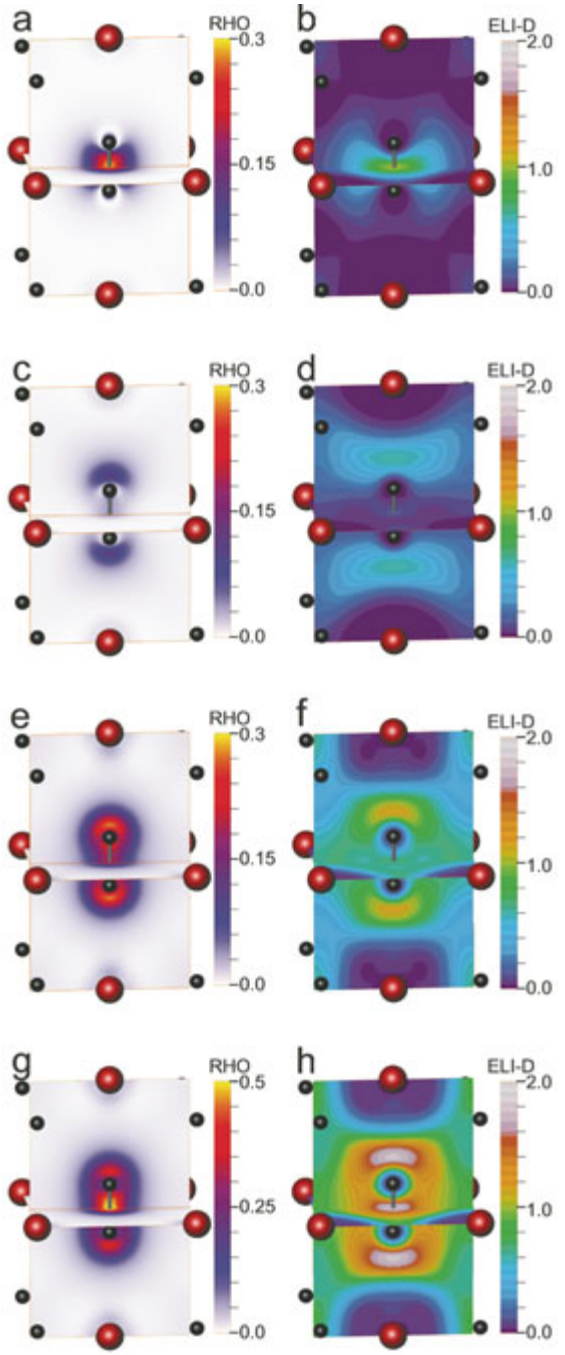

Fig. 2: CaC_2. Color-coded partial electron densities (left column) and corresponding pELI-D contributions (right column) for (a) and (b) DOS part A, (c) and (d) DOS part B, (e) and (f) DOS part C, (g) and (h) all valence electrons. Colored spheres indicate Ca (red) and C (black). For DOS parts see Fig. 1.

The obtained partial electron density and pELI-D diagrams can nicely be compared (Fig. 2). It can easily be seen that DOS part A yields C–C bonding contributions spatially concentrated in the internuclear region. From the large deviation from sphericity of the electron density around each C core a strong *s–p* mixing of this nominal C(*s*)–C(*s*) band ($2e^-$/f.u.) can be inferred. For DOS part B ($2\ e^-$/f.u.) the same process leads to the lone-pair type region displayed by pELI-D instead of simply the σ**s* antibonding orbitals. Consistent herewith, DOS part B has a low weight in COHP(C–C) displaying only tiny antibonding contributions. DOS part B yields spatially less concentrated contributions compared to part A, although both contain the same number of electrons. This becomes clear by taking into account the different characteristics of the DOS contributions: one diatomic region for part A vs. two monoatomic regions for part B. The majority of electrons ($6e^-$/f.u.) are contained in DOS part C. It displays strong contributions in the internuclear and the lone-pair region. No further features, e.g., π-type contributions which would lead to ring-shaped pELI-D contributions, have been resolved. Although it cannot be excluded that such features might indeed be resolved with a suitably chosen energy window in DOS part C, it would still be of minor interest, since no such topological feature is present in (total) ELI-D. Primarily those pELI-D features are meaningful that survive in ELI-D. All three diagrams sum up to yield the valence electrons' pELI-distribution. It displays the C–C internuclear attractor and two lone-pair type attractors at the bond-opposed side seen for ELI-D as well. The lone-pair type regions of the C_2 unit may serve as e^--donors for the Ca atoms.

The extent and the polarity of such interactions can be determined from the ELI-D/QTAIM intersection procedure (Fig. 3): the ELI-D lone-pair type basin of the C_2 units is intersected by the QTAIM atoms being displayed in Fig. 3a. As can be seen from Fig. 3b the lone pair type basin is intersected by five QTAIM Ca atoms in total: one on the C–C bond-opposed side, and four atoms surrounding the bond midpoint. The ELI-D attractor is located well inside the QTAIM carbon atom (Fig. 3a) which already signals that the lone-pair type basin mainly belongs to the C atom.

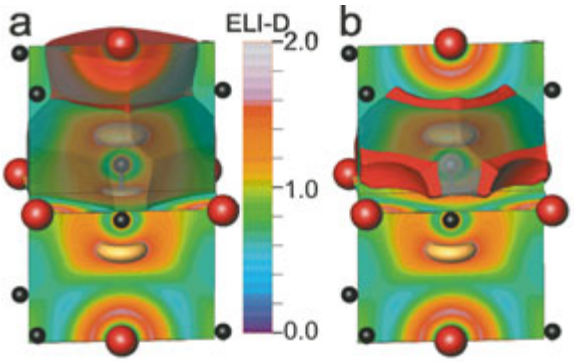

Fig. 3: CaC_2. Slices display color-coded ELI-D values according to color map; light brown ELI-D isosurfaces represent ELI-D 1.60-localization domains for C–C bond and C_2 lone-pair type basins. (a) QTAIM basins of Ca (half cut by unit cell edge) and C atoms; (b) ELI-D/QTAIM intersection of a carbon lone-pair type basin. Red intersections belong to Ca QTAIM atoms. The grey translucent region belongs to the C QTAIM atom

More quantitatively, integration of the electron density in these separate sub-basins yields that 95% (2.99 e^-) of the 3.13e^- of the lone-pair type basin belong to the QTAIM C atom. The bond-opposed Ca atom obtains 0.05e^-, the other four Ca atoms in total 0.08e^-. Thus, from this point of view, these ELI-D basins can well be classified to represent lone pairs rather than C–Ca bonds.

In a similar way, the extent of participation of the four lateral Ca neighbors in the C–C bond basin can be evaluated. In total, only 2% of the electronic basin population are contained in four Ca QTAIM atoms.

From the QTAIM partitioning effective atomic charges can be obtained. The QTAIM Ca atoms display an electronic population of 18.58e^- ($Ca^{1.4+}$), the QTAIM C atoms 6.71e^- leading to a formulation according to $C_2^{1.4-}$.

From the ELI-D partitioning of space the total number of electrons for the C_2 unit in CaC_2 is calculated yielding 2 × 2.11e^- (C core) + 2 × 3.13e^- (lone pair) + 3.26e^- (bond) = 13.7e^-. The conceptually missing 0.3e^- are found in the Ca 3rd shell which is a known chemical bonding effect. This shows that even for this quite ionic case, the electron counting for the C_2 unit using the ELI-D basin populations still misses part of the electrons compared to the formal electronic book keeping in the oxidation number procedure.

C_2 in $La_7Os_4C_9$

The crystal structure of this compound [1] is built from polymeric units $^1_\infty[Os_4(C_2)_2C_5]$ running along [101] of the monoclinic unit cell with the La species in-between (Fig. 4). The polymer is composed of alternating $Os(C_2)C_2$ and OsC_3 units with the transition metal in distorted trigonal planar coordination. The C–C distance (131 pm) within the C_2 units is slightly shorter than the value of a common double bond.

The total density of states reveals five separated DOS regions, A1, B1, A2, B2, and C (Fig. 5a). From the local DOS projections (Fig. 5b) and COHP(C–C) diagrams (Fig 5c) it is evident that regions A1, A2 and C contain electron density associated with the C_2 units, while regions B1 and B2 are related to the monoatomic C species and will not be discussed here.

The partial density and pELI-D contributions for A1, A2 and C are displayed in Fig. 6. Similar to CaC_2 the energetically lowest DOS part A1 with 4e^-/f.u. describes C–C bonds with strong mixing of C(*p*) functions into the nominal σ*s* orbitals. This results in a high accumulation of charge density in the internuclear region and a local maximum of the corresponding pELI-D distribution at the bond midpoint. DOS part A2 (4e^-/f.u.) contains the nominal σ*s states. As in CaC_2, sizable *s–p* mixing leads to the creation of a lone-pair type region. However, this situation holds only for that carbon atom C(Os) of the C_2 unit which is coordinated to an Os atom. For the other carbon atom C(La) that

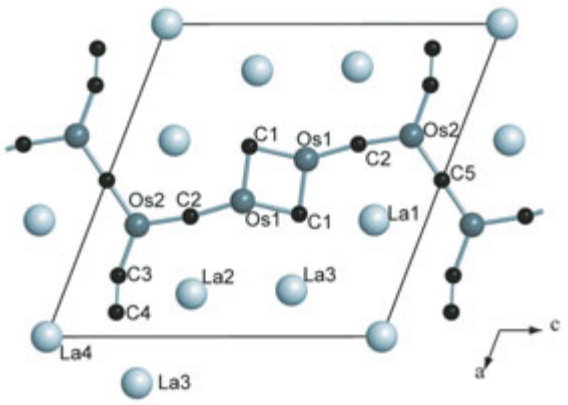

Fig. 4: $La_7Os_4C_9$. Crystal structure viewed along [010]

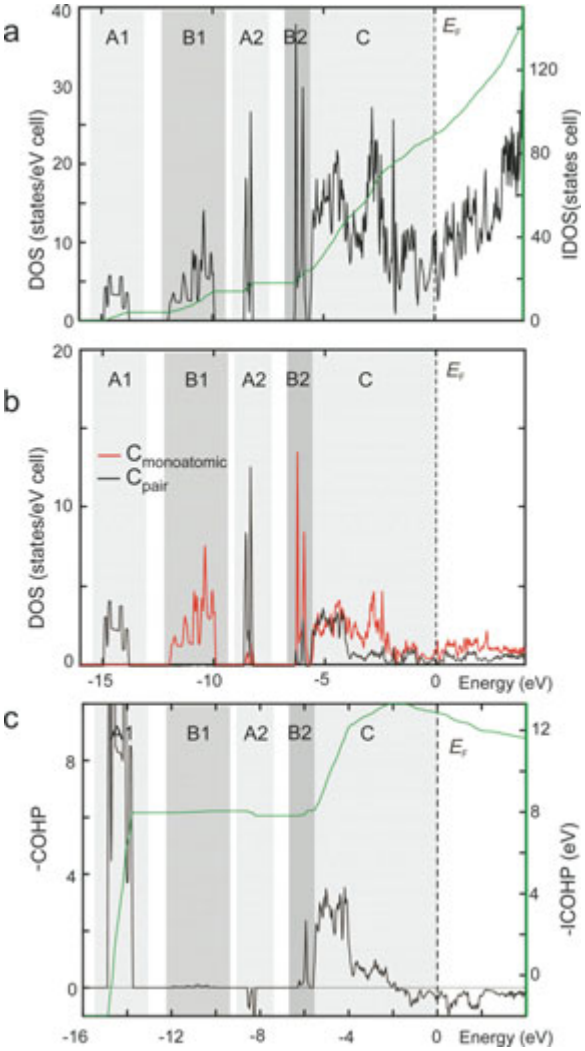

Fig. 5: $La_7Os_4C_9$. (a) total DOS, (b) local DOS projections and (c) COHP(C–C).

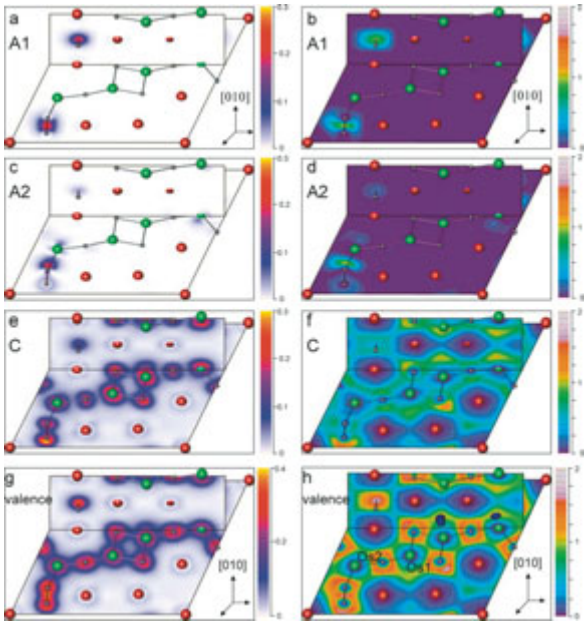

Fig. 6: $La_7Os_4C_9$. Color-coded partial electron densities (left column) and corresponding pELI-D contributions (right column) for (a) and (b) DOS part A1, (c) and (d) DOS part A2, (e) and (f) DOS part C, (g) and (h) all valence electrons. For DOS parts see Fig. 5.

is coordinated by La atoms exclusively a lone-pair type region is created as well, but by states at higher energies, i.e., DOS part C. The latter contains the majority of the valence electrons ($65e^-$/f.u. out of $89e^-$/f.u.) and yields not only C–C πp type interactions, but also metal–metal interactions the most prominent of which turned out to be of multicenter type Os–La [1]. In the valence electron pELI-D (Fig. 6h) and in (total) ELI-D (Fig. 7a-c) the described chemical features of ELI-D can be seen. The fact, that the two lone-pair type regions of the C_2 units are built from energetically different parts of the DOS points to significantly different bonding interactions C–La and C–Os. This is further evaluated using the ELI-D/QTAIM intersection procedure.

In Fig. 7a the QTAIM basins of the C_2 unit and its neighboring metal atoms within the plane are presented. The QTAIM basin of carbon atom C(La) is exclusively connected to three La atoms within the plane, while atom C(Os) is connected to two QTAIM La atoms and additionally to one QTAIM Os atom in an end-on position. Approximately above and below the bond midpoint two further QTAIM La atoms have contact with both QTAIM carbon atoms. The top surfaces of the latter have been removed in Fig. 7a to allow a better view on the ELI-D distribution inside. The result of the intersection procedure for the lone-pair type ELI-D basins is shown in Fig. 7b.

Integration of the electron density inside the displayed separate parts of the corresponding ELI-D basin yields two chemically distinct pictures for the lone-pair type ELI-D basins. The one being exclusively intersected by La atoms displays an electronic population of $3.9e^-$ of which 94% are contained inside the QTAIM carbon atom. The remaining 5% are contained within the five intersecting QTAIM La atoms. Similarly, the electronic population of the other lone-pair type ELI-D basin is $3.9e^-$. Hereof, 85% are contained within the QTAIM carbon atom. The attached Os atom cuts out 11% of the basin population, the remaining 4% belong to four attached QTAIM La atoms.

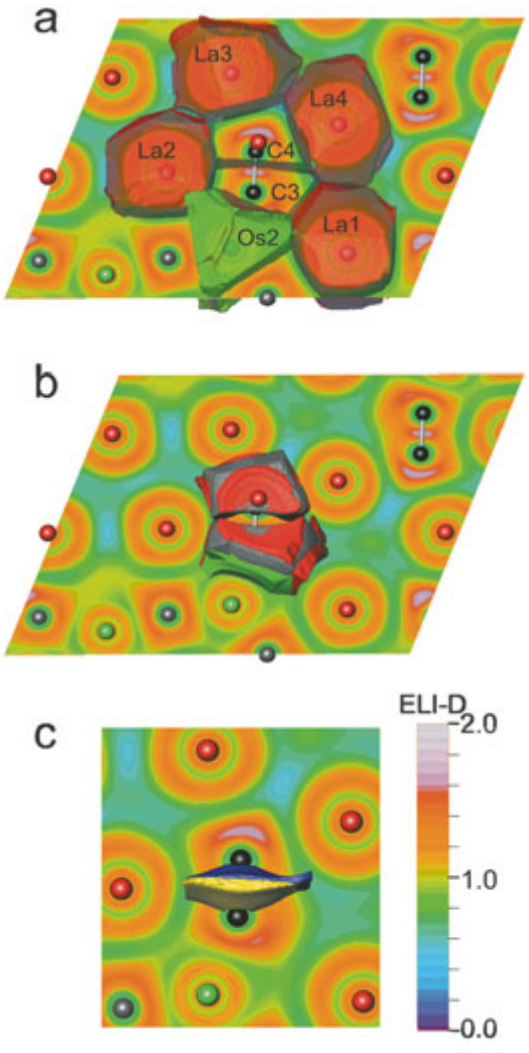

Fig. 7: $La_7Os_4C_9$. Analysis of C_2 units: (a) QTAIM basins for local environment, (b) ELI-D/QTAIM intersection of C lone pair type basins (green part belongs to QTAIM Os, red parts belong to QTAIM La atoms), (c) ELI-D/QTAIM intersection of the C–C internuclear basin.

Thus, the carbon lone-pair type ELI-D basin pointing to La atoms can be considered a "true lone pair" with negligible intersections by other atoms (1% per La on average). The other C lone-pair type basin pointing to an Os atom displays a significant intersection (11%) by the QTAIM Os atom. Consequently, it is no longer to be considered a lone pair, but a feature of a polar donor–acceptor interaction. This result is consistent with our earlier conclusions (based on COHP analyses) about the different extent of the covalent interaction between carbon and transition metal atoms compared to carbon and rare-earth metal atoms in rare earth carbometalates [8].

As a consequence of the different behavior of their "lone pairs", the carbon atoms of the C_2 unit turn out to be quite different as well. Although the QTAIM carbon atom C(Os) has "lost" part of its lone-pair population, it displays the higher QTAIM basin population of $7.2e^-$ compared to $6.7e^-$ for C(La). The reason is the very different partitioning of the bond basin population of $2.6e^-$, out of which C(Os) obtains $1.7e^-$ while C(La) obtains only $0.9e^-$. For the QTAIM atom C(Os) the "loss" of $0.3e^-$ from the lone-pair basin is overcompensated by a gain of $0.8e^-$ due to the bond basin partitioning. The emerging picture is in accord with the well accepted Dewar-Chatt-Duncanson concept in the framework of MO theory for the chemical bonding of CO (isoelectronic to C_2^{2-}) to an electron-rich transition metal. The σ-donor functionality of the coordinated carbon atom is accompanied by a π-acceptor capability, which leads to a "back-donation" of charge density and a weakening of the C–O bond due to occupation of antibonding orbitals. Interestingly, in the present case the net charge effect of the charge back-donation is stronger than that of the donation, and the metal-coordinating C atom displays the higher electronic population.

In summary, the C_2 unit is found to consist of substantially distinct QTAIM atoms, $C^{1.2-}$ and $C^{0.7-}$, which display polar homoatomic bonding with a bond basin population of $2.6e^-$. Only one of the two bond-opposed "lone-pair" type basins can really be considered a lone pair, while the other one forms a polar donor–acceptor bond with one Os atom. For an even further investigation of the bonding mechanism in position space the above mentioned delocalization indices would be very useful, but are still not available for crystalline compounds.

A chance for a classification?

From the QTAIM partitioning an effective electronic charge according to $C_2^{1.9-}$ is obtained for the C_2 units in $La_7Os_4C_9$. Although it might be tempting to take the next higher integer value, i.e. C_2^{2-}, for the formal charge assignment it should be done with caution. The reference compound CaC_2 yields $C_2^{1.4-}$ units from the QTAIM partitioning. A classification of these C_2 species according to formal C_2^{2-} can be regarded as a linear scaling (an arbi-

trary assumption) of the effective charge –1.4 by a factor of 2/1.4 = 1.43. Using this scale factor, obtained on the basis of an arbitrary assumption, for the C_2 species in $La_7Os_4C_9$ yields a scaled value of –2.7 for the effective charge –1.9, which is still closer to C_2^{2-} than to C_2^{4-}.

On the other hand, a different way of electron counting from position space partitioning can be performed using ELI-D basin populations and attributing these to one atom completely. Counting the total number of electrons for the C_2 species in $La_7Os_4C_9$ according to 2 × 2.13e^- (C core) + 2 × 3.92e^- (lone pair) + 2.56e^- (bond) = 14.7e^- reveals an excess population of 1.0e^- over the reference C_2^{2-} unit in CaC_2. Even if one neglects that for participation of transition metal atoms a higher charge transfer into the metal's penultimate shell than in the CaC_2 case would not be unexpected, this result clearly rules out the classical C_2^{2-} scenario in $La_7Os_4C_9$.

This demonstrates the difficulty to obtain from "true" charge values the conceptual, formal ones [9]. At least to date there is no fundamental prescription of how to achieve it.

The same is true for the bond order. Since it represents no quantum mechanical observable, different definitions are possible and do exist.

In MO theory the simplest definition of a bond order between atoms *X* just employs the sum of *X–X* bonding minus the sum of *X–X* antibonding orbitals. According to this, in the isolated C_2^{2-} (isoelectronic to N_2) unit no antibonding π^* orbitals are occupied, while in the isolated C_2^{4-} (isoelectronic to O_2) half of the antibonding π^* orbitals are occupied. In both molecules the σp and πp orbitals are fully occupied yielding formal bond orders of 3 and 2 for C_2^{2-} and C_2^{4-}, respectively. For the C_2 units in $La_7Os_4C_9$ the COHP(C–C) curves for the σp and the two πp interactions indicate a roughly 75% occupation of σ bonding levels and about 10% population of antibonding π^* orbitals yielding a formal bond order of about 2.5.

From the ELI-D partitioning there are found 0.8e^- more in the C_2 lone-pair type basins and 0.6e^- less in the C–C bonding basin compared to CaC_2. Calculating a type of effective bond order from the ratio between the bond basin populations of the reference and the actual C_2 unit (similar as in [7]) yields 3 × 2.56 / 3.25 = 2.4 which is roughly the same as obtained from COHP analysis. Thus, although there is only one lone pair type of attractor for each C atom of the C_2 species as in CaC_2, the C_2 species in $La_7Os_4C_9$ displays an effective bond order between that of C_2^{2-} and C_2^{4-}. Based on all these findings a classification of the present C_2 units is not attempted. Further systematic work on compounds containing C_2 units is necessary in order to establish a meaningful classification scheme.

References

[1] *E. Dashjav, Y. Prots, G. Kreiner, W. Schnelle, F. R. Wagner, and R. Kniep,* J. Solid State Chem. **181** (2008) 3121.

[2] *R. F. W. Bader,* Atoms in Molecules: A Quantum Theory, Clarendon Press, Oxford, 1990.

[3] *M. Kohout,* Int. J. Quantum Chem. **97** (2004) 651.

[4] *M. Kohout,* Faraday Discuss. **135** (2007) 43.

[5] *F. R. Wagner, V. Bezugly, M. Kohout, and Yu. Grin,* Chem. Eur. J. **13** (2007) 5724.

[6] *s. „Theoretical Aspects of Electron Localizability"*

[7] *S. Afyon, P. Höhn, M. Armbrüster, A. Baranov, F. R. Wagner, M. Somer, and R. Kniep,* Z. Anorg. Allg. Chem. **632** (2006) 1671.

[8] *E. Dashjav, G. Kreiner, W. Schnelle, F. R. Wagner, R. Kniep, and W. Jeitschko,* J. Solid State Chem. **180** (2007) 636.

[9] *W. Bronger, A. Baranov, F. R. Wagner, and R. Kniep,* Z. Anorg. Allg. Chem. **633** (2007) 2553.